A Study of Rolling-Element Bearing Fault Diagnosis Using Motor's Vibration and Current Signatures

Yang, Zhenyu; Merrild, Uffe C.; Runge, Morten T.; Pedersen, Gerulf K.m.; Børsting, Hakon

Published in:
Elsevier IFAC Publications / IFAC Proceedings series

Publication date:
2009

Document Version
Publisher's PDF, also known as Version of record

Preprints of the 7th IFAC Symposium on
Fault Detection, Supervision and Safety of Technical Processes
Barcelona, Spain, June 30 - July 3, 2009

A Study of Rolling-Element Bearing Fault Diagnosis Using Motor's Vibration and Current Signatures

Zhenyu Yang * **Uffe C. Merrild** * **Morten T. Runge** *
Gerulf Pedersen * **Hakon Børsting** **

* *Department of Electronic Systems/Esbjerg Institute of Technology, Aalborg University, Niels Bohrs Vej 8, 6700 Esbjerg, Denmark*
** *Grundfos A/S, Poul Due Jensens Vej 7, 8850 Bjerringbro, Denmark*

Abstract:
This paper investigates the fault detection and diagnosis for a class of rolling-element bearings using signal-based methods based on the motor's vibration and phase current measurements, respectively. The envelope detection method is employed to preprocess the measured vibration data before the FFT algorithm is used for vibration analysis. The average of a set of Short-Time FFT (STFFT) is used for the current spectrum analysis. A set of fault scenarios, including single and multiple point- defects as well as generalized roughness conditions, are designed and tested under different operational conditions, including different motor speeds, different load conditions and samples from different operating time intervals. The experimental results show the powerful capability of vibration analysis in the bearing point-defect fault diagnosis under stationary operation. The current analysis showed a subtle capability in diagnosis of point-defect faults depending on the type of fault, severity of the fault and operational condition. The generalized roughness fault can not be detected by the proposed frequency methods. The temporal features of the considered faults and their impact on the diagnosis analysis are also investigated.

1. INTRODUCTION

The bearing component plays a critical role in rotational machines, its functionality is directly relevant to the operational performance, and consequently the reliability and safety of these machines and relevant systems. Benbouzid [2000] discovered that over 40% of induction motor failures are due to bearing component faults. Thereby some cost-effective early Fault Detection and Diagnosis (FDD) of potential bearing faults is very important and necessary when it comes to reliable operation of a given system.

A standard rolling-element bearing consists of an inner and outer raceway with a set of balls or rolling-elements placed between these two raceways and held by a cage (Changsen [1991]). As shown in Fig.1, bearing faults could happen with the raceways, ball or rolling-element and the cage as well, such as a scratch on the surface of the raceway(s). The bearing faults can be caused due to improper installations of the bearing onto the shaft or into the housing, misalignment of the bearing, contamination, corrosion, improper lubrication, brinelling or simply due to wear-out (Benbouzid [2000], Li et al. [2000]). Stack et al. [2004] classified bearing faults into two general categories: single-point defects and generalized roughness. A single-point defect is defined as a single, localized defect on a bearing component surface. Generalized roughness corresponds to the situation where the condition of a bearing surface has degraded considerably over a large area, and become rough, irregular, or deformed.

Extensive research work can be found focusing on the FDD of the single-point defect, due to the fact that a single defect will produce one of the four characteristic fault frequencies depending on which bearing component contains the fault. The most popular way to detect these characteristic frequencies is to use the vibration measurement of the motor shaft plus advanced signal processing techniques. The Fast Fourier Transform (FFT) is the natural choice to retrieve frequency features from measured stationary time-domain data. Theoretically, the single-point fault characteristic frequencies can be predicted based on the shaft speed and the bearing geometry. By comparing the spectra generated based on a nominal operation and a fault-suspected operation around these characteristic frequencies, if some obvious difference can be observed, the corresponding fault scenario will be claimed. In order to cope with potential non-stationary situations, e.g., due to the change of shaft speed during the measuring period, Tse et al. [2001] proposed a method using the Wavelet method to analyze the vibration signal so as to tradeoff the time-frequency resolution. Li et al. [2000] proposed a Neural-Network-based diagnosis method so as to cope with potential uncertainties and nonlinearities ignored by theoretical analysis. There is no doubt that these methods can provide an enhanced and more powerful capability for bearing fault diagnosis compared to conventional spectrum methods, however, the following critical issues need to be overcome before these methods can be extensively put into industrial applications:

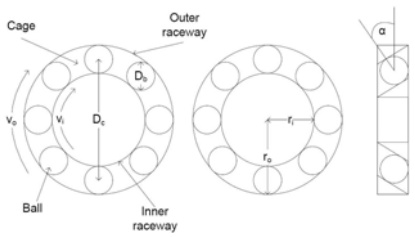

Fig. 1. Scheme of a standard rolling-element bearing

- A systematical way to select an appropriate set of parameters for analysis;
- Complexity and computation load.

Instead of using the vibration measurement, another option is to use the phase current measurement from the induction motor (Benbouzid and Kliman [2003], Schoen et al. [1995], Yazici and Kliman [1999]). However, so far there is only a few results on the use of this method for bearing fault diagnosis (Benbouzid and Kliman [2003], Stack et al. [2004]).

The FDD of generalized roughness defects is nearly blank in research literature, even though this kind of fault is common in industry. The difficulty of this problem lies in the fact that there are no characteristic fault frequencies reflected by the current or vibration signals associated with this type of fault (Stack et al. [2004]). Some model-based methods might be helpful in solving this problem.

Motivated by our purpose for the possible extensive industrial application, hereby our work intends to use some simple and commercially off-the-shelf methods for the study of bearing FDD. Therefore the FFT-based methods are employed for vibration and current signature analysis, respectively. The envelope detection method is employed to preprocess the measured vibration data before the FFT algorithm is used for vibration analysis. The average of a set of Short-Time FFT (STFFT) is used for the current spectrum analysis. A set of fault scenarios, including single and multiple point- defects as well as generalized roughness conditions, are designed and tested under different operational conditions, including different motor speeds, different load conditions and samples from different operating time intervals. Especially, the feasibility of using the current signature analysis for potential bearing FDD is quite interesting to our industrial partner, because many pump systems (called E-pump systems) produced by Grundfos A/S already have the motor current measured inside the integrated control module which is apparently used by the pump controller so as to control the pump performance. If possible, it would be quite cost effective to use the already available motor current instead of installing extra vibration sensors for the bearing FDD purpose. Meanwhile, the integration of the developed FDD algorithm into the existing control module is quite straightforward.

The paper is organized in the following: Section 2 describes the considered testing setup and apparatus; Section 3 states the theoretical analysis of fault characteristic frequencies; Section 4 presents the results derived from vibration and current signature analysis under different testing scenarios; Section 5 discusses the results and presents some preliminary studies of the temporal features of concerned faults and their impact on the developed FDD analysis; and finally we conclude the paper in Section 6.

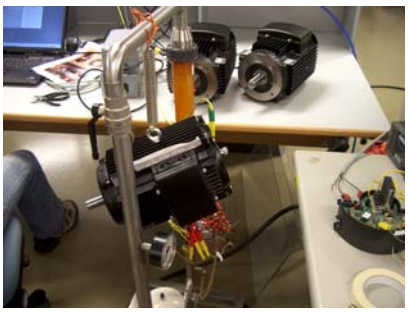

Fig. 2. The induction motor with its suspension system

2. TESTING SETUP AND APPARATUS

A type of 3- kW three-phase induction motor (MG100LC2-28FT130-D1) is used in our tests. This type of motor has two bearings with different sizes, the big one is mounted at the load end of the shaft, the small one is at the back end of the motor. The load side bearing is considered for fault detection and diagnosis. An accelerometer (W352B10) produced by Piezotronics is used to measure the vibrations of the motor. This type of sensor has a frequency range of 1 - 10000Hz and can measure a peak acceleration up to $4900m/s^2$, while one piece only weighs 0.7 gram. The selected accelerometer is quite sensitive, and the 4294 Brüel & Kjær calibrator is thereby used to calibrate all sensors before they are deployed on the motor setup. The measurements of the phase current is carried out by standard electrical equipment. In order to determine the motor shaft speed, a hand-held optical tachometer is used. The data acquisition is handled by the Brüel & Kjær Dyn-X 3560B 5 channel data recorder. For the vibration measurements, the data recorder sets up a high-pass filter with a cutoff frequency of 7 Hz in order to remove all possible DC offsets. The sampling rate is selected as 16384 Hz. The ISO 10816 Standard is followed for selection of accelerometer position. The bearings used in this study are NSK 6305. A set of defective bearings are artificially designed so as to study different fault scenarios. The data processing and analysis are mainly carried out in Matlab. More details can be found in Merrild and Runge [2006].

The motor setup is arranged into three different configurations in order to study the possible influences due to different external loads:

- *Free-load setup* - The motor runs free without any external load and hence no cooling fan inside the housing;
- *Fan-load setup* - The cooling fan is attached on the motor shaft; and
- *Pump-load setup* - The motor setup (with fan) is placed in a water circulation system and is used to drive a Grundfos CR-8 centrifugal pump.

In order to minimize the impact from the surrounding environment on the motor vibration dynamic, as shown in Fig.2, the induction motor is suspended on a spring for the first two configurations. The third configuration can be seen in Fig.3.

Fig. 3. The induction motor in a circulation system

3. FAULT SCENARIOS AND THEIR CHARACTERISTIC FREQUENCIES

3.1 Fault Scenarios

Along with a set of healthy bearings, one defective bearing is designed to have a scratch on the inner raceway, which services as an (single-point) inner raceway defect scenario. The second defective bearing has a hole with a diameter of 3mm through the outer raceway and a scratch on the outer raceway as well. The second bearing services as a (multi-point) outer raceway defect scenario. This type of fault is used to emulate an extremely serious (multiple) point-defect situation. The third defective bearing is designed without lubricant, so that it services as a generalized roughness condition. The FDD algorithms are tested for different scenarios under different operating conditions:

- Three different load configurations;
- Different motor speeds;
- Data sampled from different operating intervals.

Both the vibration analysis and phase current analysis are carried out and compared in the following.

3.2 Vibration Characteristic Frequencies

It is well known that the single-point defect can produce four predictable characteristic fault frequencies based on the knowledge of the bearing's geometry and motor shaft speed (Benbouzid [2000], Li et al. [2000]), i.e.,

$$\begin{aligned} F_c &= \frac{1}{2}F_s(1-\frac{D_b cos\alpha}{D_c}) \\ F_{ri} &= \frac{N_b}{2}F_s(1+\frac{D_b cos\alpha}{D_c}) \\ F_{ro} &= \frac{N_b}{2}F_s(1-\frac{D_b cos\alpha}{D_c}) \\ F_b &= \frac{D_c}{2D_b}F_s(1-\frac{D_b^2 cos^2\alpha}{D_c^2}) \end{aligned} \quad (1)$$

where the *cage fault frequency*, F_c, is the frequency with which the ball passes a defective cage point; *Inner/outer raceway fault frequency*, F_{ri}/F_{ro}, is the frequency with which the ball passes a defective inner/outer raceway point, F_b/F_s is the ball/motor-shaft rotational frequency. N_b is the number of balls, D_b/D_c is the diameter of the ball/cage, and α is the contact angle between the raceway and balls. It should be noticed that this prediction is based on the assumption of pure rolling races, however, in reality, some sliding motion may occur which causes deviations of characteristic frequencies (Tse et al. [2001]).

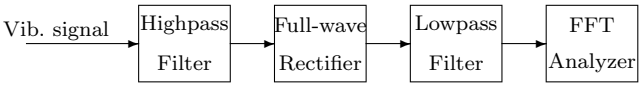

Fig. 4. Envelope detection (DLI Engineering Corp)

3.3 Envelope Detection

As mentioned by Tse et al. [2001] the envelope detection technique needs to be used together with FFT in order to make the characteristic frequencies more distinguished from the noise spectra. We use the envelope detection method as shown in Fig.4. For our considered case, the cutoff frequency of the high-pass filter is selected as 2500 Hz. The signal is then passed through a full-wave rectifier in order to demodulate the vibration signal, and finally a low-pass filter is used to filter out the higher harmonics of the signal, where the low-pass filter is used with a cut-off frequency of 500 Hz. Both filters are implemented as FIR filters with the order of 200 in Matlab.

3.4 Current Characteristic Frequencies

The bearing faults can also possibly be detected via motor current measurements (Benbouzid and Kliman [2003]). A bearing defect will normally produce a radial motion between the rotor and stator. This mechanical displacement will cause variations of the air gap flux density inside the motor. This changing air gap flux consequently causes the stator currents to vary at the *current characteristic frequencies* which can be predicted as

$$F_{ccf} = |F_s \pm mF_{i,o}|, \quad (2)$$

where $m = 1, 2, 3, \cdots$, $F_{i,o}$ is one of the vibration characteristic frequencies specified in (1).

4. TEST RESULTS AND ANALYSIS

The considered bearing FDD is based on the checking of the spectrum magnitudes around characteristic frequencies. By comparing with a nominal bearing spectrum, if some large magnitude deviations can be observed around some specific characteristic frequencies, then the corresponding fault scenario will be claimed. The tests are carried out under different conditions so as to study the influence of different external loads, shaft speeds and environments to the FDD analysis. Due to the page limitation, some selected results are presented in the following. More details can be found in (Merrild and Runge [2006]).

4.1 Vibration Analysis - Point-defect, Free-load, Different Shaft Speeds

The considered motor is controlled by a frequency converter, thereby speeds of the motor is denoted as 50 Hz, 40 Hz and 20 Hz (inputs to the frequency converter), respectively. One set of spectra based on the 50 Hz motor speed and radial position measurements is shown in Fig.5. It can be easily seen that both the inner raceway fault and outer raceway fault show significant features compared with the nominal bearing spectrum, whose overall level is around 27 dB. Similar results are also observed by the axial data analysis as well as the results with 40 Hz speed measurements Merrild and Runge [2006].

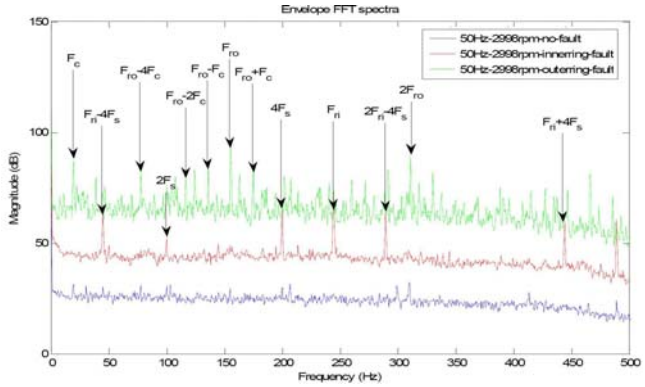

Fig. 5. Spectra of 50 Hz, free load, radial vibration

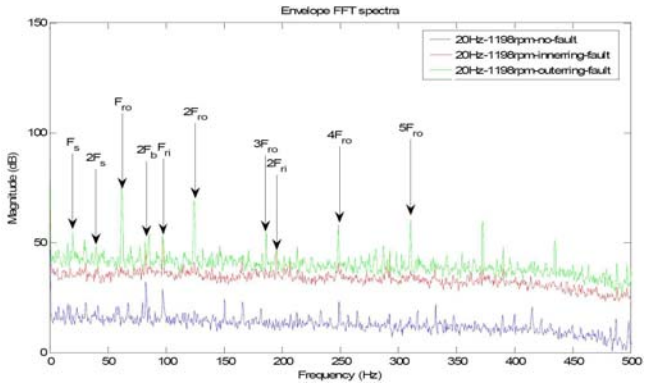

Fig. 6. Spectra of 20 Hz, free load, axial vibration

A set of spectra based on the 20 Hz motor speed and axial position measurements is shown in Fig.6. It can be observed that all resonance peaks for different fault scenarios are much smaller compared with situations with 50 Hz and 40 Hz motor speeds (which is not shown here due to the page limit). However, both fault scenarios can still be clearly detected. The tests with different shaft speeds exhibit that the shaft speed does impact on the vibration levels and the actual characteristic frequencies do change to their theoretical values with small deviations corresponding to the shaft speed changes.

4.2 Vibration Analysis - Point-defect, 50 Hz input, different load conditions

When the pump-load setup is tested, the actual shaft speed is measured at 48.96 Hz. Regarding the inner raceway fault, a set of spectra based on the radial position measurements is shown in Fig.7. It can be observed that this fault scenario can be detected for all three load conditions. The spectra of the free-load and fan-load are quite similar, while the spectrum of the pump-load is different from the others in terms of small peaks and small observable deviations of characteristic frequencies (mainly due to the actual shaft speed) from the predicted ones.

Regarding the outer raceway fault, a set of spectra based on the radial position measurements is shown in Fig.8. This fault scenario can be detected for all three load conditions. It is interesting to observe that the spectrum with pump-load does not suppress the peaks much around the characteristic frequencies, this is different from the inner raceway fault situation. This observation could be

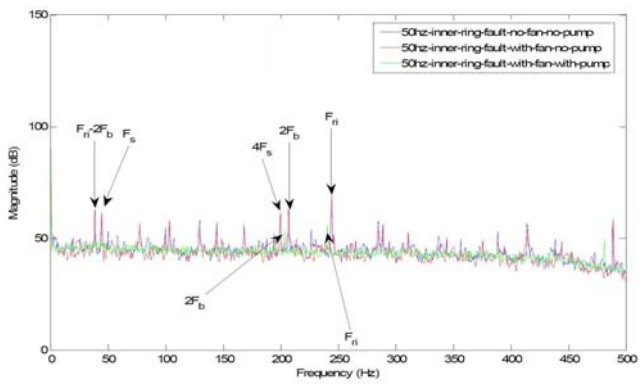

Fig. 7. Spectra of 50 Hz input, radial position, different loads, inner fault, vibration measurements

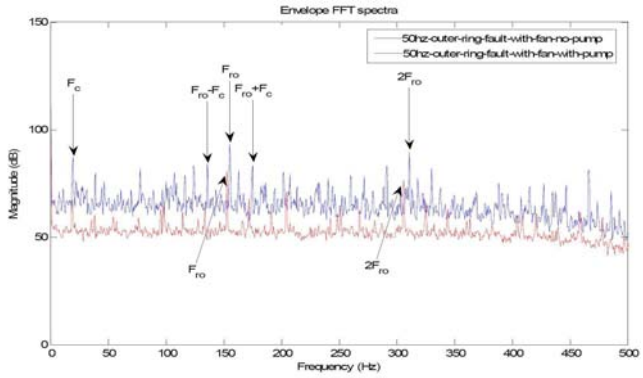

Fig. 8. Spectra of 50 Hz input, radial position, different loads, outer fault, vibration measurements

mainly due to the centrifugal phenomenon and a large outer raceway fault (multiple-point defects) as well.

4.3 Vibration Analysis - Generalized Roughness, 50 Hz input, different load conditions

A bearing without lubricant is used to test the FDD analysis under a generalized roughness situation. A set of spectra based on the radial position, 50 Hz input and different load conditions is shown in Fig.9. There is little difference between the spectra of free-load and fan-load conditions. There are some small peaks in these two spectra. However, no peak is over 48 dB. As shown in Fig.5, the peak for the inner raceway fault frequency can reach 74 dB, therefore, no point defect can be claimed based on the observation in Fig.9. The spectrum of the pump-load is even more flat than the others.

4.4 Current Analysis - Point-defect, Free-load, 50 Hz Shaft Speed

One phase current is measured and used for the bearing FDD analysis. One mean STFFT spectrum of the current measurements under the same operational condition as studied in Section 4.1 is shown in Fig.10 and Fig.11, respectively. Some harmonics of fault characteristic frequencies can be observed in different ranges. However, the amplitudes of harmonics of the inner raceway fault quickly decrease along with the increasing frequency. Whereas the amplitudes corresponding to outer raceway fault become

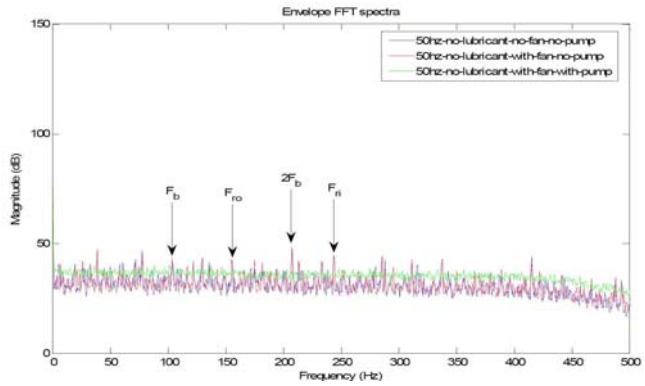

Fig. 9. Spectra of 50 Hz input, radial position, different loads, no lubricant, vibration measurements

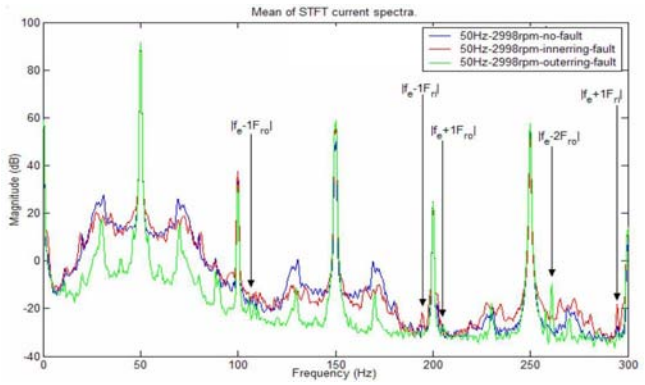

Fig. 10. Spectra of 50 Hz speed, free load, radial current measurements (0-300 Hz)

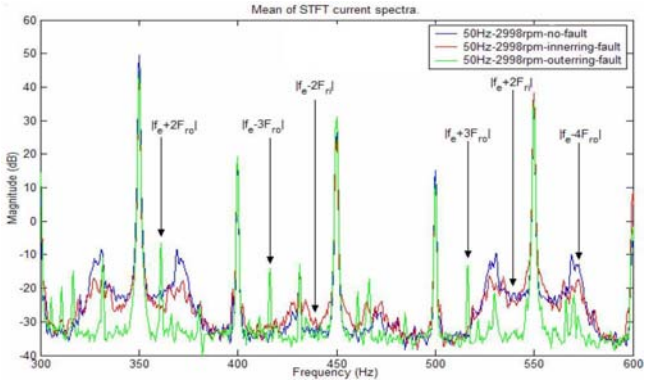

Fig. 11. Spectra of 50 Hz speed, free load, radial current measurements (300-600 Hz)

more distinguished for the high frequency range. Comparing with the vibration analysis in section 4.1, it is obvious that the FDD based on current analysis can not reach the same significant level as vibration analysis does.

4.5 Current Analysis - Point-defect, 50 Hz input, different load conditions

A set of current spectra from 300-600 Hz under the same operational conditions as studied in Section 4.2 is shown in Fig.12. It can be seen that it is difficult to detect the inner raceway fault for the free-load and fan-load conditions. However, the inner raceway fault frequencies

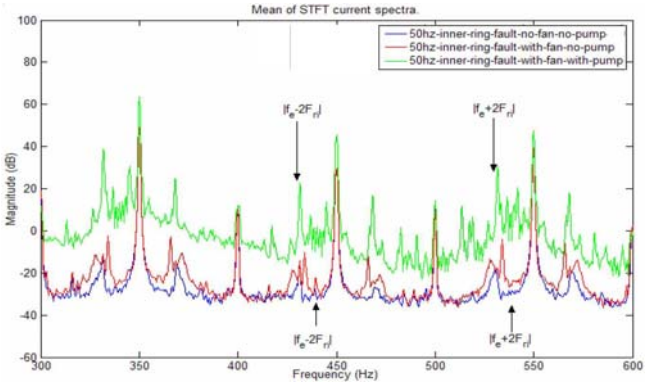

Fig. 12. Spectra of 50 Hz input, radial position, different loads, inner fault, current measurements

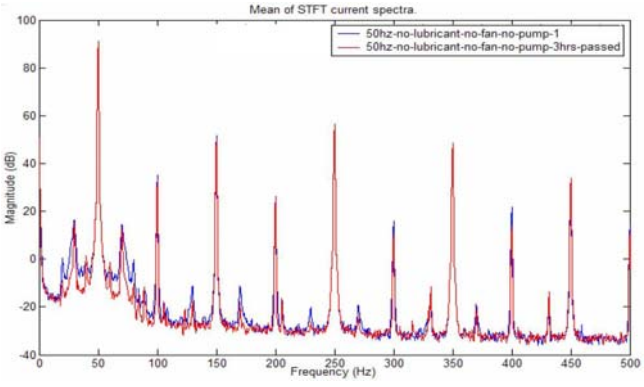

Fig. 13. Spectra of 50 Hz input, radial position, different loads, no lubricant, current measurements

appear clearly in the pump-load spectrum, it indicates the detectability for this fault scenario.

4.6 Current Analysis - Generalized Roughness, 50 Hz input, different load conditions

A set of current spectra under the same operational conditions as studied in Section 4.3 is shown in Fig.13. It can be seen that there is no possibility to detect this type of fault through current signature analysis either.

5. DISCUSSIONS

In general, the vibration analysis showed a significant power in detection and diagnosis of bearing point-defects. However, the current spectrum analysis did not reach what we expected at the beginning. Among all the designed scenarios, the outer raceway fault can be detected for different motor speeds and different load conditions as well. the inner raceway fault can only be clearly detected for the pump-load condition. Some investigation using phase current signature for motor rotor and stator fault diagnosis can be found in Benbouzid and Kliman [2003]. One option to possibly improve our current signature analysis is to use a notch filter to get rid of the 50 Hz and its harmonics before the current measurement is transformed (Benbouzid and Kliman [2003]). Furthermore, the usage of some more precise current measurement techniques and some more advanced signal processing techniques, could also be helpful in improving the spectrum resolution and

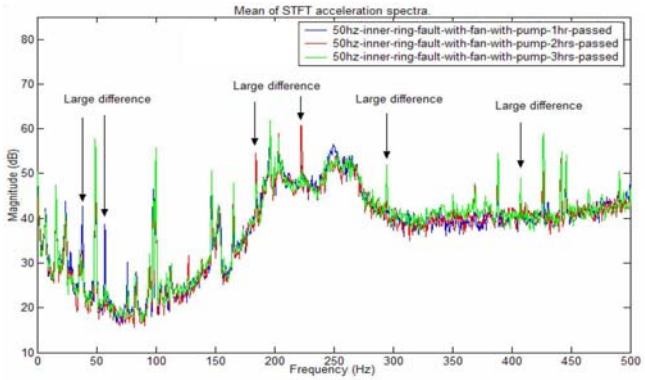

Fig. 14. Spectra of 50 Hz radial pump-load vibration measurements, inner fault, with one hour interval

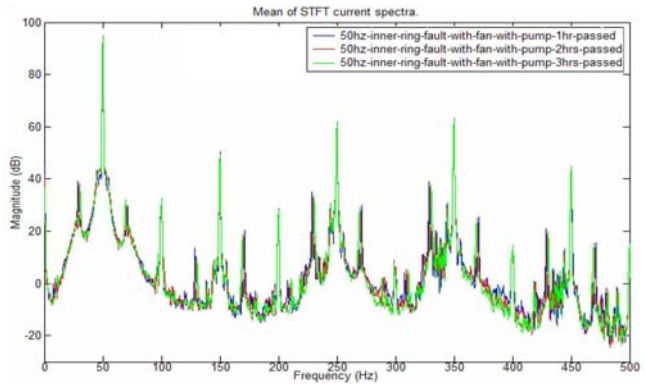

Fig. 15. Spectra of 50 Hz radial pump-load current measurements, inner fault, with one hour interval

handle possible non-stationary or aperiodic measurements. Nevertheless, whether a better results can be obtained or not fundamentally depends on the significance level of the considered bearing fault features reflected in the current measurement. In order to get a deeper insight into this problem, some model-based analysis might be necessary.

Some temporal features of considered bearing faults and their influences to FDD analysis are also investigated in our work. A set of vibration spectra based on data sampled from different motor running time intervals is shown in Fig.14, and the current spectra are shown in Fig.15. Some differences (peaks) due to different motor running time can be observed in the vibration spectra, while these differences are not visible in the current spectra. A study of the no-lubricant fault is shown in Fig.16. The temporal development of this type of fault can be clearly observed. The overall vibration level is significantly increased as the motor runs for a long time. It indicates that some adaptive threshold is required if the overall significance level is used for detection (Yazici and Kliman [1999]).

6. CONCLUSION

The bearing fault diagnosis is investigated by using FFT-based methods based on vibration and the current measurements, respectively. Most of the point-defect scenarios can be diagnosed via the vibration signature analysis. The current signature analysis can detect the designed outer raceway fault under different scenarios, but it can only detect the designed inner raceway fault under the pump-

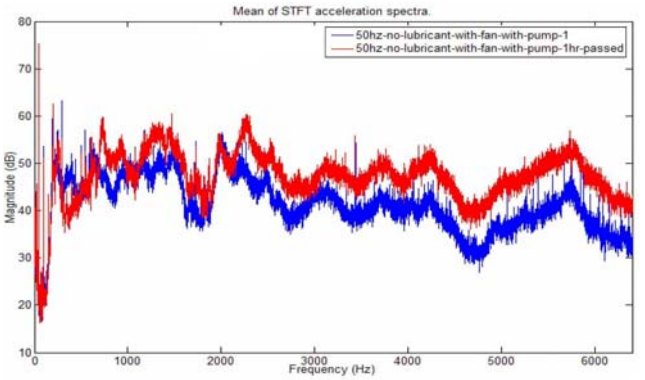

Fig. 16. Spectra of 50 Hz radial pump-load measurements, no lubricant with one hour interval

load configuration. Nevertheless, this configuration is quite common in industrial systems. Thereby this work shows a huge potential to use a simple current signature analysis for diagnosis of industrial bearing systems.

ACKNOWLEDGEMENTS

The authors would thank Grundfos A/S for initiating the project and providing testing facilities and technical supports.

REFERENCES

Mohamed El H. Benbouzid. A review of induction motors signature analysis as a medium for faults detection. *IEEE Trans. on Industrial Electronics*, 47(5):984–993, 2000.

W. Changsen. Analysis of rolling element bearings. *Mechanical Engineering Pub. Lmited, London*, 1991.

Mohamed El H. Benbouzid and Gerald B. Kliman. What stator current processing-based technique to use for induction motor rotor faults diagnosis? *IEEE Trans. on Energy Conversion*, 18(2):238–244, 2003.

Bo Li, Mo-Yuen Chow, Y. Tipsuwan and James C. Hung. Neural-network-based motor rolloing bearing fault diagnosis. *IEEE Trans. on Industrial Electronics*, 47(5): 1060–1069, 2000.

Randy R. Schoen, Thomas G. Habetler, Farrukh Kamran and Robert G. Bartheld. Motor bearing damage detection using stator current monitoring. *IEEE Trans. on Industry Applications*, 31(6):1274–1279, 1995.

Jason R. Stack, Thomas G. Habetler and Ronald G. Harley. Fault classification and fault signature production for rolling element bearings in electric machines. *IEEE Trans. on Industry Applications*, 40(3):735–739, 2004.

Peter W. Tse, Y.H. Peng and Richard Yam. Wavelet analysis and envelope detection for rolling element bearing fault diagnosis - their effectiveness and flexibilities. *Journal of Vibration and Acoustics*, 123:303–310, 2001.

Uffe C. Merrild and Morten T. Runge. Detection of bearing faults in induction motors. *Master Thesis, Aalborg University*, 2006.

Birsen Yazici and Gerald B. Kliman. An adaptive statistical time-frequency method for detection of broken bars and bearing faults in motors using stator current. *IEEE Trans. on Industry Applications*, 35(2):442–452, 1999.